The Role of Bulk Charge Transport Processes in Electrical Tree Formation and Breakdown Mechanisms in Epoxy Resins

N. M. Chalashkanov, S. J. Dodd, L. A. Dissado,
University of Leicester
University Road
Leicester, LE1 7RH

and **J.C. Fothergill**
City, University of London
Northampton Square
London, EC1V 0HB

ABSTRACT

Electrical treeing experiments have been conducted at different temperatures and levels of absorbed moisture in Araldite CY1311 epoxy resin samples above their glass transition temperature, i.e. when the resin was in a flexible state. The fractal dimension of the electrical trees obtained and the rate of tree growth were found to depend on the environmental factors: temperature and humidity. It has also been found that at certain levels of temperature and moisture absorbed in the samples, a transition occurs from electrical treeing degradation to breakdown by thermal runaway. Complementary investigations of the dielectric properties of the same epoxy resin system have revealed that a bulk quasi-dc (QDC) charge transport mechanism takes place above the glass transition temperature, and we show that the characteristic features of the dielectric response are related to the shape of the electrical treeing degradation and the transition to thermal breakdown. This is explained qualitatively through the effect of the bulk QDC charge transport process in modifying the local space charge electric field distribution.

Index Terms — **Epoxy resins, electrical breakdown, electrical trees, charge transport, thermal breakdown**

1 INTRODUCTION

ELECTRICAL treeing is a pre-breakdown degradation mechanism that is initiated by local high stress points such as metallic asperities, discharging voids [1], and water trees [1, 2]. It leads ultimately to electrical breakdown [1], once the tree has crossed the insulation. Electrical tree propagation is governed by partial discharges (PDs) occurring in the tree channels, or in the case where the channels gain a thin graphitic conducting layer at the top of the channels [3, 4]. The shape of the electrical trees can be characterized by their fractal dimension, d_f [1, 3]. Two main categories can be identified according to the tree fractal dimension, namely branch trees with $1<d_f<2$ and bush trees with $2< d_f < 3$. In some cases a bush tree develops a small number of long branched structures extending from its periphery and is called a bush-branch tree, whose overall fractal dimension can be taken as $d_f \approx 2$. In epoxy resins electrical tree growth has been found to depend on various factors, including applied electric stress [5, 6], frequency of the applied voltage [7], temperature [8], absorbed moisture [9], material state (rubber-like or glassy) [4], and others.

Several models of electrical tree growth have been proposed in the literature, which can be broadly classified into two main categories: deterministic and stochastic [3]. Stochastic models assume a step-wise tree growth and rely on a random selection of the direction of each tree channel addition which has been justified either on the basis of material inhomogeneity [10] or random local variations in the factors that control the damage mechanism that eventually results in a new channel. The stochastic models have an ability to create fractal structures similar to those experimentally observed. The main criticism of the stochastic models is that they do not provide sufficient understanding of the physical processes governing the growth of electrical tree structures (for example the process of partial discharge induced damage, branch formation and bifurcation), although some physical parameters can be included in such models, for example the dc conductivity of the bulk dielectric material was incorporated in [11]. Furthermore a semi-deterministic model [12] has shown that random material inhomogeneity did not lead to fractal trees, but produced structures dominated by weak paths. Structures more akin to fractals were formed only when factors influencing the local electric fields were varied dynamically according to a random selection from a specified distribution. The development of fully deterministic models for electrical tree growth and corresponding PD activity

has allowed a detailed study of the factors influencing the tree growth [3, 4, 13-15]. Unlike the stochastic models, the deterministic models resolve the spatial distribution of the PDs within the tree structure based on a given set of physical parameters and electrostatic boundary conditions, and generate damage using quantitative physical factors related to the PD. The conductivity of tree walls was introduced as a model parameter in [4] and the calculated PD magnitudes showed a significant dependence on this parameter. The model outcomes reflect the experimental observations where conductive and non-conductive electrical tree structures were found [16].

Space charge is produced in the vicinity of the tree structure as a result of the PD activity. The effect of these space charges has been incorporated in a deterministic Discharge Avalanche Model (DAM) [14]. The results of the model suggest that the fractal dimension of the resultant tree structure depends upon the availability of electrons for back avalanches, the amount of charge produced in each discharge, the fraction of charges that recombine when brought together during a time-segment, and less strongly on the initial value of the minimum distance needed for impact ionization [14]. Other factors such as the recombination of positive and negative charges also contribute in determining the shape of the tree structures. According to DAM, a reduction of charge recombination and increased electron availability of electrons for back-avalanches gives bush structures, while increasing recombination and reducing electron availability eventually gives straight punctures [14].The amount of space charge available around the tree structure is also dependent on the bulk charge transport mechanisms in the dielectric material, which were incorporated into [14] by allowing injected and avalanche-generated carrier to penetrate the polymer beyond the damage region at the growing tree tips under the action of the local electric field. However most of the existing models do not account for the influence of the environmental factors (temperature and relative humidity) on the growth of the electrical degradation.

In this work we have used the dielectric measurements presented in [17] to determine that there is a bulk quasi-dc (QDC) transport process that is available to displace charges in a set of flexible epoxy resins. The analysis allows us to determine the conditions of humidity, temperature, and frequency, under which the displacement of the charge will be effective in moving discharge-injected charge away from electrical tree tips during the half-cycle of an applied voltage. The modification of the electric field distribution around the tree periphery produced in this way has resulted in a qualitative explanation of the influence of temperature, absorbed moisture, and frequency of the applied voltage on electrical tree propagation and tree shapes observed in electrical treeing experiments on the same resins [18].

2 EXPERIMENTAL

2.1 SAMPLE PREPARATION

The cured epoxy resin system was prepared by mixing the base epoxy resin Araldite CY1311 with 30% by mass amine hardener Aradur HY1300GB. The glass transition temperature of this resin is 0 °C, and all tests were performed above T_g of the resin i.e. with the resin in its rubbery state. The liquid epoxy resin and hardener were first degassed in a vacuum oven in separate beakers for 10 min at 30 °C to 40 °C. Then they were mixed together on a hot plate (~40 °C) using a magnetic stirrer for 10 min. After mixing, the mixture was degassed in the vacuum oven for 10 min to remove any air bubbles trapped during the mixing stage. Aluminium molds were used to produce plaque samples in two thicknesses: 0.7±0.1 mm and 1.7±0.1 mm for dielectric measurements. For the electrical treeing experiments tungsten pins having shank diameter 1 mm and radius of curvature 3µm were cast in epoxy slabs of size 50 mm x 20 mm x 5 mm with a pin-plane distance of approximately 2 mm.

All samples were left to cure in their molds for two days at room temperature (~20 °C). They were then post-cured for 1 h at 100 °C under vacuum to ensure completion of the cure reaction before slowly cooling down to room temperature. The samples, assumed dry at this stage, were then weighed using an analytical balance of 0.1 mg precision before being stored in sealed containers under controlled temperature (20 °C) and relative humidity (using saturated salt solutions). Saturated salt solutions of LiCl, $MgCl_2$, K_2CO_3, and NaCl or de-ionized water were used to create environments with a stable relative humidity of 15, 30, 44, 75 and 100% respectively at room temperature [19, 20].

2.2 DIELECTRIC MEASUREMENTS

A bespoke test cell, shown in Figure 1, was used for the dielectric measurements. This was designed to enable dielectric measurements to be taken in a controlled temperature and humidity environment in order to maintain a stable level of absorbed moisture in the samples over a sufficient length of time to enable the dielectric measurements to be made. A three-electrode configuration was used for the measurements. Further details of the test cell and the measurement equipment used can be found in [17].

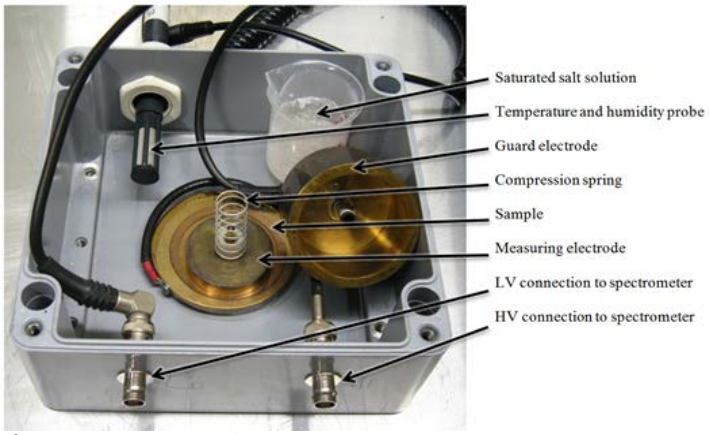

Figure 1. A photograph of the measurement cell [17].

2.3 ELECTRICAL TREE EXPERIMENTS

A set of experiments have been carried out to establish the influence of temperature and moisture on electrical degradation mechanisms related to electrical treeing in epoxy resins. A standard pin-plane electrode configuration was used for the

treeing experiments. The electrical treeing experiments were conducted 2-3 months after the samples were manufactured, and all samples were conditioned in sealed containers with different levels of relative humidity over that period. The mass uptakes of the samples were recorded by measurements with the analytical balance. All samples were produced using the same manufacturing procedure and stored in the same sealed containers as described above, so direct comparison between the results obtained from the dielectric measurements and the treeing experiments was possible.

The experiments were carried out in a Faraday cage to exclude external electromagnetic interference. The pin-plane electrode geometry samples were contained within a glass cell filled with silicone fluid to eliminate discharges occurring along the surface of the sample during the tests. A HV transformer rated at 20 kV rms provided the 50 Hz applied voltage, which was connected to the pin electrode. The brass base-plate of the glass cell formed the plane electrode, which was connected to earth potential.

The electrical trees were grown at 13.5 kV rms, 50 Hz ac applied voltage and the apparent charge was measured using a RCL resonant circuit coupled to the HV circuit using a high voltage discharge free coupling capacitor. A RCL circuit having a resonant frequency of 200 kHz was used and the PD amplitudes and phase angles with respect to the ac applied voltage were recorded by a digital storage oscilloscope (DSO). The minimum sensitivity of this measurement system was 1.5pC. The data acquisition interval was 1 s with 10 s time delay between consecutive acquisitions. A cartridge heater embedded in the cell base-plate and controller allowed the treeing experiments to be conducted at chosen fixed temperatures in the range 20-70 °C. The treeing cell was thermally insulated so that a constant temperature was maintained in the cell during the tests. A Peltier-cooled CCD camera was used to monitor the tree structure during growth using back-illumination to capture images of the electrical trees.

3 RESULTS

3.1 DIELECTRIC MEASUREMENTS

The dielectric response of a CY1311 sample at different temperatures is shown in Figure 2. The sample was conditioned in a container with saturated solution of LiCl (RH 15%) and the level of absorbed moisture in the sample was 0.1%. All spectra are obtained for the resin above its T_g. The spectra given in Figure 2 shift to higher frequency with increasing temperature. It was possible to obtain master plots for both the temperature and humidity dependence of the dielectric response by translating the data along the log frequency and log amplitude axes to bring the response plots into coincidence (equivalent to rescaling the characteristic frequency and amplitude). A master plot of the dielectric spectra given in Figure 2 with the addition of 30 °C and 50 °C data, is shown in Figure 3. The locus of the translation point is given below the master curve and the spectra are normalized with respect to the data obtained at the highest temperature. As previously reported the dielectric spectra exhibits a quasi-dc (QDC) process and a mid-frequency dispersion [17]. The QDC behavior implies that in these conditions charge transport takes place by means of structured paths [21] that are not uniformly distributed spatially.

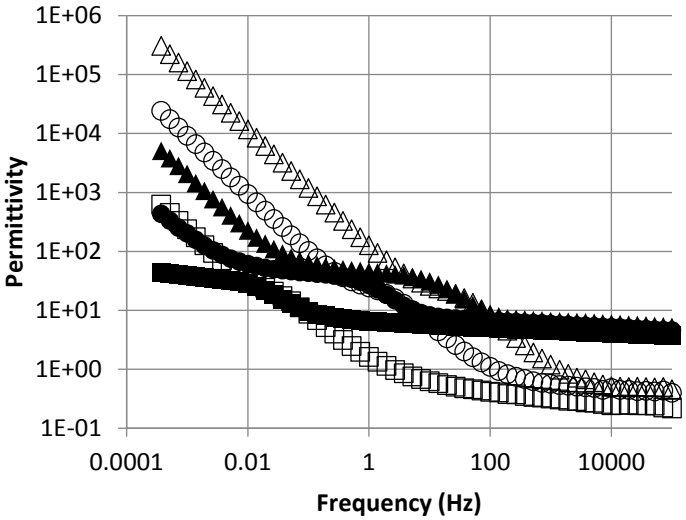

Figure 2. Real (filled) and imaginary (open markers) components of the relative permittivity of epoxy resin CY1311 at 20°C(■), 40°C(●), and 60°C(▲), absorbed moisture 0.1%, sample thickness 0.8 mm

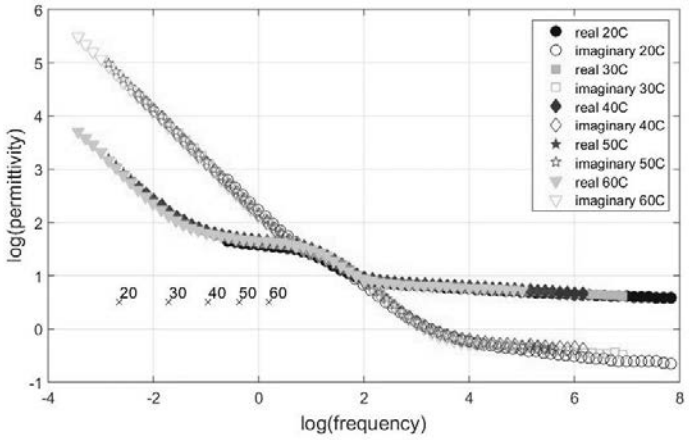

Figure 3. Master plot of the temperature dependence of CY1311 sample, absorbed moisture 0.1%, thickness 0.8mm

The humidity dependence of the dielectric spectra of four samples, conditioned in environments with RH 15%, 30%, 75% and 100% and having mass uptakes prior to the dielectric measurements of 0.2%, 0.7%, 3.0%, and 7.2%, respectively is shown in Figure 4. The locus of the translation point is given below the master curve and the spectra are normalized with respect to the highest humidity data. In this case, the high frequency ends of spectra appear to coincide, however there are some differences in the mid and low frequency regions. The increment of ε' associated with the mid-frequency dispersion appears to have amplitude that varies from sample to sample. In the low frequency region, the real and imaginary parts of the permittivity for samples with a high water content do not run parallel to each other as expected from a QDC response [21]. Instead the slope of ε'' is equal to -1, while ε' has a slope greater than -1, which varies from sample to sample. This form of behavior has been described in [22], where it is shown that it originates with the charging of a dispersive electrode interface

capacitance by a bulk DC conductance. The interface capacitance in this case is usually assumed to be an electrical double layer that permits diffusion, anomalous or otherwise. Since such a double layer is very thin compared to the sample thickness it has a very large capacitance and the apparent permittivity estimated from the measurements can reach extremely large values that increase gradually at very low frequencies where the diffusion takes effect. The spectra in Figure 4 suggests that this form of behavior occurs in samples with higher water content, i.e. that the high water content converts the QDC behavior observed in low water content samples into a spatially uniform DC conductance.

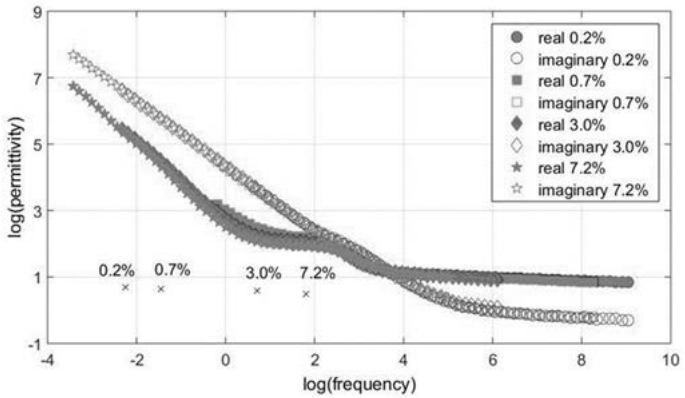

Figure 4. Master plot of the humidity dependence of CY1311 samples, temperature 30 °C, thickness 1.7mm

The dielectric measurement data for samples without sputter-coated gold electrodes were fitted using the equivalent circuit proposed in [17]. This is reproduced in Figure 5. The bulk material is modelled by QDC_1 and QDC_2. The interface is modelled by a series blocking capacitance, C_s, which represents the air-gap in the case of imperfect contact, and a conductance, G_s, inserted in parallel with C_s to represent surface conduction along the epoxy surface. Typical values of the characteristic parameters for a sample with a level of absorbed moisture 0.2%, thickness 1.7 mm are given in Table 1 for different temperatures. These values were obtained from the dielectric data by a non-linear least squares fitting procedure to the equivalent circuit. The value of the frequency independent capacitance C_∞ was assumed to be 18 pF, which corresponds to a relative permittivity of $\varepsilon_{r\infty} = 2.3$ [17].

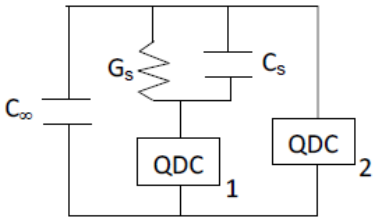

Figure 5. Equivalent circuit used for fitting the dielectric data [17]

An important question that has not yet received an answer is that of the nature of the charge carriers involved in the QDC process in the epoxy resins. Frequently, QDC is associated with ion transfer between neutral clusters leading to an extended charge separation on a percolation structure. The charges may however also be electronic in nature [21, 23].

Table 1. Fitted values, absorbed moisture 0.2%, thickness 1.7 mm

Parameter	Temperature				
	20°C	30°C	40°C	50°C	60°C
QDC1 amplitude, pF	100 ±27	12 4±3	13 5±2	149 ±2	154 ±2
QDC2 amplitude, pF	55 ±27	34 ±3	20 ±2	14 ±1	9 ±1
Low frequency slope (p)	-0.976 ±0.001	-0.972 ±0.001	-0.969 ±0.001	-0.971 ±0.001	-0.974 ±0.001
High frequency slope (n-1)	-0.088 ±0.004	-0.092 ±0.002	-0.092 ±0.002	-0.090 ±0.003	-0.086 ±0.004
QDC characteristic frequency, Hz	1.1 ±0.1	9.3 ±0.2	59 ±2	278 ±11	1056 ±47
C_∞, pF	18	18	18	18	18
Gs, DC conductance (interface), pS	1.0 ±3.7	28 ±4	243 ±20	1175 ±80	4232 ±257
C_S, Series capacitance, pF	382 ±238	630 ±35	815 ±34	917 ±36	966 ±37

In hydrated biopolymers [24-26], which have been found to have a similar dielectric response to that of the epoxy resin presented in Figure 4, it was suggested that proton transfer is responsible for the long-range charge transport QDC mechanism, and some evidence for isotope dependence has been presented in [25] supporting this hypothesis. The chemical composition of the epoxy resin systems also has the potential for proton transfer, with proton donors, such as salicylic acid, often being used to facilitate polymerization and accelerate the final curing reaction [27] between hardeners such as diamine and the epoxide groups. Its presence in the epoxy used here is supported by the GC/MS analysis presented in [28].

The role of the salicylic acid in the epoxy system is complicated and may result in more than one type of ion. It may react in the presence of amine groups giving a mono-anion and the acid group thus formed may open the epoxide group ring. There is also a possibility that some salicylic acid exists in the hardener as mono-anions or as di-anions assuming that additional proton donation may occur. The concentration of both species will depend on the equilibrium conditions. In addition a condensation reaction involving salicylic acid and hydroxyl groups may occur during the cure reaction [27], when the concentration of hydroxyl groups is increased due to the opening of the epoxide ring. This reaction can account for the presence of initial moisture after the epoxy samples have been post-cured as reported in [28]. Thus the presence of salicylic acid may be a necessary prerequisite for proton donation and consequently proton transfer between hydrogen bonded water clusters, which would give rise to the observed QDC behavior.

Figure 6 shows the dissociation of a salicylic acid molecule in the presence of water. The consequent proton transfer can be understood in terms of “structural diffusion” [29] in which a topological defect migrates through the hydrogen-bonded system rather than an actual mass diffusion of either protons H+ or H3O+ protonic complexes. This process requires the simultaneous breaking and making of covalent bonds in interchange with making and breaking of the associated hydrogen bonds due to changes in the orientation of the

molecules involved in the hydrogen-bonded network. In this way the proton can be effectively transferred through the cluster as shown in Figure 6. It should be noted that a negative charge created by the removal of a proton from a water molecule can also be transferred through the H-bond connected water molecule sequence in a similar way. In this case it is still a proton that moves in a H-bond, but now it is a negative charge that is effectively transported.

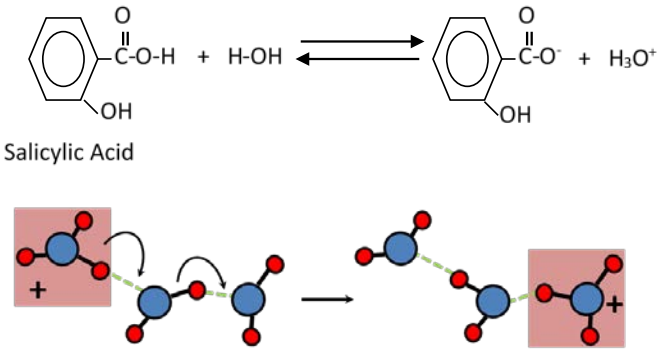

Figure 6. Proton donation and transport in epoxy resins. (Top) Dissociation of salicylic acid in the presence of water. (Bottom) Proton transfer along a cluster of hydrogen bonded water molecules from [29]

As can be seen in Figure 4 absorbed water strongly facilitates the QDC by reducing the time required for the transfer of charge carriers between one cluster and another i.e. increasing ω_c. The anomalous diffusion observed in the dynamics of water absorption in epoxy resins [9] suggest that the absorbed water is present in both bound and mobile states, and in a recent study on water diffusion in epoxy systems using deuterium NMR analysis [30] it has been suggested that the mobile water is comprised of H_2O molecules interacting with the polymer network while the bound water occurs as a result of the formation of water molecule clusters.

Since there is no detectable charge transport below T_g while above T_g it has a high activation energy ~1.5eV [17] it is likely that the long range charge transport associated with the QDC behavior at $\omega < \omega_c$ requires significant segmental motions of the polymer network. Consequently the transfer of charges between clusters in the QDC mechanism has to be associated with the water molecules that are attached to the polymer, i.e. the mobile fraction, which possibly transfer protons when segmental chain motions transiently form water molecule chains as in Figure 6 leading to dynamic charge percolation on structured paths. It is also possible that the amine groups in the hardener chains play a role as these have a high proton affinity [31] and are therefore likely proton hopping sites albeit ones with a substantial activation energy. A high enough moisture content would raise the system above the percolation limit giving rise to a true DC conductance.

Charge displacements produced as a result of these bulk transport processes would give rise to dynamic variations of the local electric field and could be of importance for electrical degradation in epoxy resins [32]. They would also occur during an electrical treeing experiment where local field fluctuations are important in determining the tree shape [3], and could be of importance in explaining the effect of moisture on tree shape in epoxy resins [9].

3.2. ELECTRICAL TREEING EXPERIMENTS

The effect of absorbed moisture on the electrical treeing process is illustrated in Figure 7, where images of four trees grown at applied voltage of 13.5 kV rms and T = 20 °C in samples with moisture levels of 0.1%, 1.0%, 2.4%, and 6.9% are shown in a) to d), respectively. The images shown in Figure 7 were taken after the end of the corresponding experiment and represent the final tree structures obtained [18]. The fractal dimension of the final tree structures was estimated using a MATLAB program based on the box counting method applied to the image which is a 2D projection of the tree. As long as the tree has a fractal dimension less than 2 this method gives an acceptable value. In the case of the tree image in Fig.7a, the body of the tree is completely black indicating a region where no light can penetrate and therefore has a fractal dimension greater than 2. Such a value cannot be estimated properly by this method. Instead the program includes the open branch structure on the tree periphery to give an average value over the whole image of 1.8. In reality this tree is a bush-branch tree with a genuine fractal dimension greater than 2.

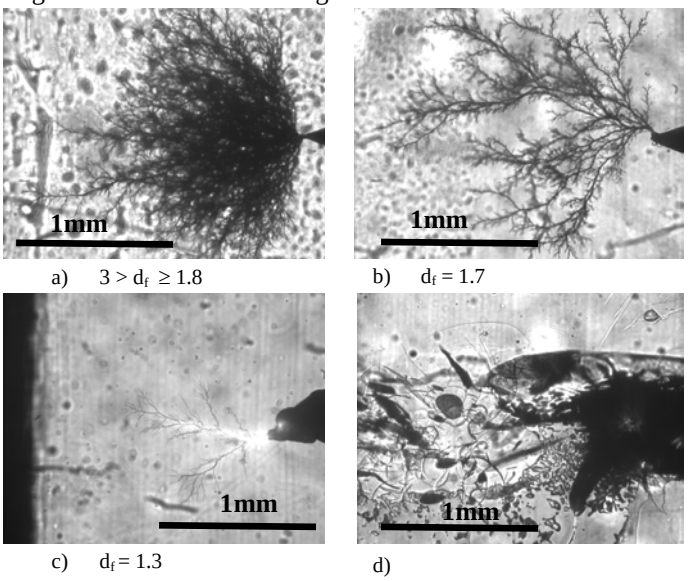

a) $3 > d_f \geq 1.8$ b) $d_f = 1.7$

c) $d_f = 1.3$ d)

Figure 7. Electrical degradation and breakdown at different levels of absorbed moisture, temperature 20°C, applied voltage 13.5kV rms, pin-plane distance 2mm: moisture level of: a) 0.1%, b) 1.0%, c) 2.4%, d) thermal breakdown at 6.9%. [18]

The fractal dimension of the electrical trees decreased with increasing level of absorbed moisture from a value greater than 1.8 at 0.1 % to 1.3 at 2.4%. In the sample with the highest level of moisture, Figure 7(d), the degradation mechanism had changed from electrical treeing to thermal breakdown. In this case the protection fuse of the HV transformer blew as the applied voltage was increased at the beginning of the experiment. The damage showed no tree channels and instead striations were observed indicating differing material density caused by high current flow and the production of high temperature. This is consistent with the process of thermal breakdown. A similar picture was observed when the effect of the temperature was considered at a constant level of absorbed moisture. Images of four electrical trees grown at different temperatures are shown in Figure 8. The respective samples were conditioned in a sealed container with RH 30% and had acquired about 0.6% mass increment prior to the treeing

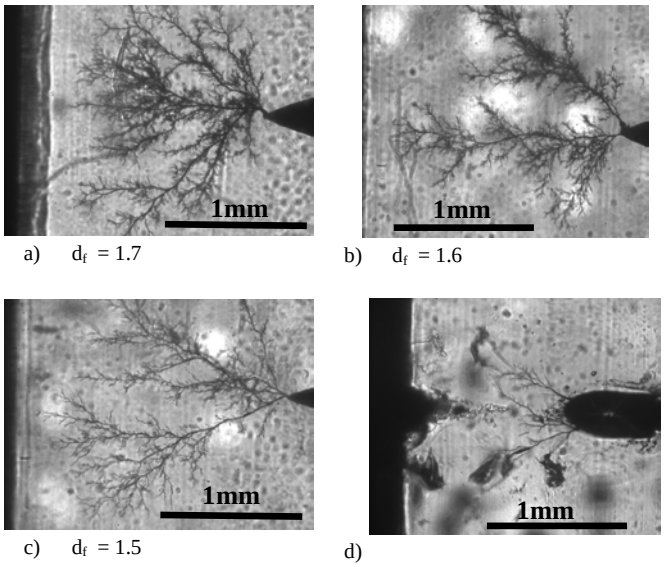

a) d_f = 1.7 b) d_f = 1.6

c) d_f = 1.5 d)

Figure 8. Electrical degradation and breakdown at different levels of temperature, absorbed moisture 0.6%, applied voltage 13.5kV rms, pin-plane distance 2mm; a) temperature 20°C , b) 30°C , c) 40°C , d) combination of treeing and thermal breakdown at 50°C . [18]

Table 2. Tree growth time

	20ºC	30ºC	40ºC	50ºC	60ºC	70ºC
RH15 (0.1%)	51min	17min	>40s	4min	2min	30s
RH30 (0.6%)	7min	3min	3min	10s	B	B
RH44 (1.0%)	7min	1min	45s	B	B	B
RH75 (2.4%)	30s	B	B	B	B	B
RH100 (6.9%)	B	B	B	B	B	B

B – breakdown (the sample broke down in less than 10s)

experiments. The fractal dimension of the trees shown in Figure 8 decreased with increasing temperature. At temperatures above 50 °C thermal runaway was observed.

In general, increasing temperature and/or moisture led to faster tree growth and lower fractal dimension of the corresponding electrical trees. Although the overall mechanism of electrical treeing did not change (PD driven phenomenon), the details of the PD dynamics were found to change significantly with increased temperature and moisture content. At even higher values of temperature and moisture, it was possible to identify a set of values for which the degradation mechanism (electrical treeing) changed to a breakdown mechanism (thermal runaway). The electrical tree growth times and the conditions at which breakdown took place are given in Table 2. Once again, the experiments were terminated before the trees were able to bridge the pin and the plane electrodes. This was done mainly to preserve the tree shapes and also to protect the RLC load circuit from possible damage. In the case of RH15 at 40 °C the experiment was deliberately terminated at 40s because of a very rapid initial growth, which prevented an accurate estimation of the tree growth time. However in some cases sample breakdown happened very quickly, i.e. less than 10s after the voltage application, and no tree images were recorded in this period of time. These cases are designated in Table 2 by the letter 'B' and thermal breakdown is assumed to be a likely breakdown mechanism given its observation in some of the other cases.

Table 3 and Table 4 give the average number of discharges per second and the average discharge magnitudes, respectively, measured over the entire tree growth, for the same set of conditions as listed in Table 2. In the cases where thermal breakdown had occurred, no PD data were collected. At low temperature and low moisture the average values of both discharge rates and magnitudes are typical of those characterizing the PD activity during the electrical tree growth [33, 34]. However, at high values of temperature and/or humidity the average PD magnitudes decrease, while the corresponding number of PDs per second increases significantly. Under the same conditions, the corresponding tree growth times are very short and indicate a runaway process [13]. In the runaway process the growth of the tree structure rapidly propagates to the counter electrode and the typical decelerating phase of tree growth [13] was not observed. Hence, the PD rates can be used to differentiate between the two regimes of electrical treeing and runaway. The runaway tree growth regime marks the transition between conventional tree growth behavior and thermal runaway breakdown. The rapid tree growth may be the result of joule heating causing the local temperature in the sample to increase above the cell temperature.

Table 3. Average number of discharges per second [s^{-1}] during the entire tree growth [34]

	20ºC	30ºC	40ºC	50ºC	60ºC	70ºC
RH15 (0.1%)	691	1164	1821	2715	11670	16850
RH30 (0.6%)	1010	1928	3496			
RH44 (1.0%)	1085	3291	18094			
RH75 (2.4%)	14258					
RH100 (6.9%)						

Table 4. Average discharge magnitude [pC] during the entire tree growth [34]

	20ºC	30ºC	40ºC	50ºC	60ºC	70ºC
RH15 (0.1%)	252	236	226	218	81	5
RH30 (0.6%)	241	182	232			
RH44 (1.0%)	336	153	68			
RH75 (2.4%)	98					
RH100 (6.9%)						

4 DISCUSSION

4.1. EFFECT OF BULK CHARGE TRANSPORT ON THE ELECTRICAL DEGRADATION AND BREAKDOWN IN EPOXY RESINS

When the characteristic frequency ω_c of the QDC process is greater than the frequency of the applied voltage, charge transport between clusters can take place during an AC half-cycle. This leads to the separation of charges between super-clusters that form part of an extended percolation system. Consequently the polarization associated with the QDC that gives rise to the increasing value of ε' towards lower frequencies, will correspond to charge separation over long distances which increase as frequency reduces. This can have a significant effect on the electrical tree growth. The charge deposited at the tips of the electrical tree as a result of the PD activity can be effectively transferred deeper into the material by this mechanism, and as a result the field within the tree structure is increased on the same half-cycle as the initial charge depositing PD. The negative feedback of the PD-deposited space charge in inhibiting successive discharges in the same half-cycle and in the same tree tube (channel) is thus ameliorated. Consequently partial discharge in the existing channels and the electrical tree growth is favored in the pin-plane direction, resulting in faster growing trees with smaller fractal dimension.

Thermal breakdown occurs when the values of ω_c are much higher than the frequency of the applied voltage (50Hz) (see Table 1). Thus it appears that the critical factor for the transition from electrical treeing pre-breakdown degradation to thermal breakdown is the length of the percolation path over which charges can be separated, and hence the PD deposited space charge can be transferred. This is consistent with a suggestion that in epoxy resins an increase in the ionic conductivity at temperatures above T_g and at high moisture levels may lead to thermal breakdown even at moderate electric fields [35]. In Table 5 we give values for tanδ at 50 Hz obtained from the raw dielectric response data. A comparison with Table 2 shows that the transition to thermal breakdown occurs when the effective (AC) conductivity of the resin exceeds a critical value which is dependent on temperature and absorbed moisture. In this particular case the transition appears to take place when tanδ is between 1 and 2. It should be noted that this will be the case when a QDC process dominates the response with ω less than about 0.1 ω_c, since then tanδ =cot((1-p)π/2) with p > 0.5 in $\varepsilon'' \propto \varepsilon' \propto \omega^{-p}$ [22].

4.2. EFFECT OF BULK CHARGE TRANSPORT ON THE PD PROCESS

Due to the bulk charge transport, the electrical charges deposited by the discharge can be moved away from the tree structure and, as a result, the local space charge field, which on the same half-cycle opposes the applied field, will be reduced. Thus another PD can take place shortly after the first one had occurred and overall more discharges occur over one half-cycle of the applied voltage.

Figure 9 shows a simplified equivalent circuit model that was used to study the effect of bulk charge transport on the gas discharges. The circuit represents a void in series with the bulk of the material. The void is represented as a spark gap in parallel with G_V, where G_V is the surface conductance of the void. A capacitor C_B in parallel with a conductance G_B represents the bulk capacitance and conductance of the epoxy resin, respectively. This model can be used for simulation of the PD activity either in the case of an electrode-bound void or as an approximation to an electrical tree, if the entire tree structure is assumed to discharge simultaneously. The PD inception E_{on} and extinction E_{off} fields were separately defined for each half-cycle of the applied stress E_{AC} as free parameters. The values of E_{on} and E_{off} have to be similar for both polarities of the applied voltage in order to mimic the PD activity in electrical trees.

Table 5. Tanδ at 50Hz as a function of temperature and absorbed moisture

	20ºC	30ºC	40ºC	50ºC	60ºC	70ºC
RH15 (0.2%)	0.08	0.10	0.15	0.35	1.00	1.29
RH30 (0.7%)	0.11	0.17	0.42	1.30	2.85	-
RH75 (3.0%)	1.14	1.96	1.92	3.40	6.45	-
RH100 (7.2%)	1.7	5.40	33.9	109	167	-

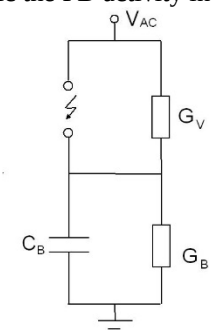

Figure 9. Equivalent circuit for PD simulation

Figure 10 shows on the left the phase-resolved plots and on the right the Pulse Sequence Analysis (PSA) return maps obtained from two calculations over 50 cycles of the applied voltage at two different values of the conductance G_B. The value of value of G_V was set to zero to model electrical tree channels that are non-conducting and the value of C_B was chosen to be 2.2nF. In both cases the peak value of the sinusoidal applied stress was 19.6 kV/mm, and the values for E_{on} and E_{off} were 11.6 kV/mm and 10.9 kV/mm for the positive polarity and 11.3 kV/mm and 10.7 kV/mm for the negative polarity respectively, since the treeing process is essentially symmetric with respect to the voltage polarity [33]. A study of the PD inception and extinction voltages and stresses in voids in different insulating materials can be found in [36]. In the phase-resolved plots, the PD pulses are indicated by the green lines, the voltage across the spark gap is given in black, the voltage across the insulation (capacitor C_B) in red and the applied sinusoidal voltage in blue. The differential ratio dU/dt

was used to analyze the simulated data and to obtain the PSA plots in the same way as the experimental data presented in [34].

The simulations resemble closely the experimental data given in [34] and reproduced here in Figure 11. In the case of a lower conductivity of the bulk resin (Figure 10a) the PDs occur in the first (Q1) and third (Q3) quadrants of the applied voltage and the PSA return map consists of six clusters, which have a similar appearance and alignment to the case of burst type behavior during an electrical tree growth, shown here on the left in Figure 11 and in [34]. The PD activity between the bursts is characterized by a significant scatter in the PSA clusters and it is not possible to simulate it using the equivalent circuit of Figure 9. In this phase of activity the tree fractal dimension has been found to increase, which implies multiple discharge sites and lower correlation between the individual PD events.

An increased bulk conductivity of the resin leads to an increase in the number of PDs per cycle and a shift in the phase window over which the PDs occur (see Figure 10b). Hence, they take place in phase with the applied voltage and even after the positive and negative voltage peaks, i.e. the negative discharges occur in Q1 and Q2, and the positive discharges in Q3 and Q4, respectively in Figure 10b. This is reflected in the corresponding PSA return map, where the clusters associated with positive and negative PD distributions extend along the 45° line. Similar return maps were observed in the cases of runaway growth, shown here on the right in Figure 11 and in [34]. The simulation therefore associates runaway growth with a high bulk conductivity for which the circuit model of Fig.9 applies throughout the discharging, i.e. the sample conductivity is nearly homogeneous throughout the bulk resin.

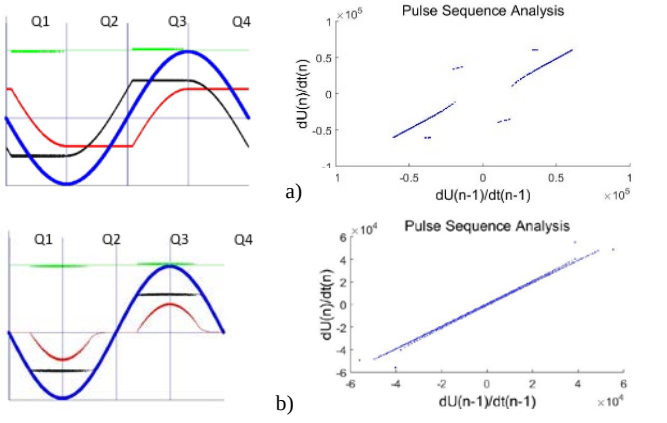

Figure 10. PD simulation over 50 cycles of the applied voltage, phase resolved data (left): PD pulses – green, applied voltage waveform – blue, voltage across the spark gap – black, voltage across the insulation – red; Pulse Sequence Analysis (PSA) plot (right); a) $G_B = 5x10^{-11}S$; b) $G_B = 5x10^{-6}S$

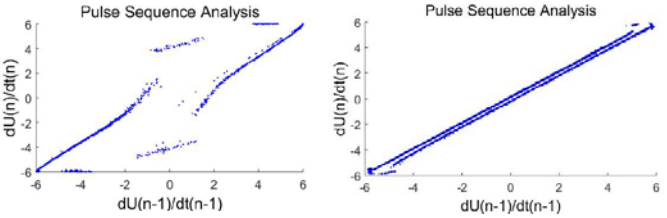

Figure 11. PSA return plot: absorbed moisture 1.0%, temperature 20°C (left) and absorbed moisture 2.4%, temperature 20°C (right) [34]

The circuit element G_B is a reasonable approximation in this case and the transition in the PD activity from typical electrical tree growth to runaway growth is associated with a high effective bulk conductivity at the frequency of the applied AC field. At low temperature and moisture content, however, the effective bulk conductivity of the resin is low and a QDC charge transport should be considered rather than DC conduction. The QDC charge transport and the underlying cluster model are usually understood in terms of fractal circuits [37-39]. The equivalent circuit in Figure 9 does not account for the fractal geometry of the electrical tree structure and the build-up of local space charges. Therefore, it does not provide sufficient complexity to mimic the real world situation. The influence of the QDC process on the electrical treeing is discussed in the next section.

4.3 A QUALITATIVE DESCRIPTION OF THE EFFECT OF BULK CHARGE TRANSPORT ON ELECTRICAL TREES

The deterministic model for electrical trees [14] made allowance for the effect of discharge generated space charge upon tree propagation. It was found that the space charge deposited around a tree channel/tubule tip inhibited further discharges in that tube and favored discharges and hence discharge-generated damage at other tips. In addition electron injection by any subsequent discharges in the same channel/tubule would be directed by the local field to produce damage in an alternative direction to that of the first discharge, thereby encouraging bifurcation. Consequently PD-deposited space charge that remains around the tree tips can be expected to lead to heavily branched trees. Since the penetration of PD-deposited charge in [14] was restricted to three grid bonds (= 30μm) because of limitations on computer time, the injected charge did not move far away from the tree tips, and thus the simulations [14, 15] always produced heavily branched trees although it was found that they could take either a branched or bush form according to the applied voltage.

The PDs calculated from the simulations of [14, 15] showed both the large bursts of activity upon branch formation [5] and also the signature of deterministic chaos [40] observed experimentally. In the present work PD simulations (Fig.10) show that under the same conditions of low dc conductivity i.e. little or no charge penetration into the bulk, the pulse sequence behaves substantially as observed experimentally for branch trees with high fractal dimension ($1.7 < d_f < 2$) and bush type trees ($d_f \geq 2$) (Fig. 11) consistent with the tree simulated in [14,15].

The charge penetration can be correlated with the moisture and temperature conditions by means of the dielectric response which shows a QDC charge transport in most cases. Here the key feature is the time, $(\omega_c)^{-1}$ at which charges are transferred between clusters, i.e. separated over distances greater than a cluster correlation length ξ_c. Since ξ_c is likely to be less, and probably much less, than the average length of a branch addition (~10μm as in [14]) the PD deposited space charge and that developed in damage generating processes such as avalanches, space charge will not be transferred very far into

the bulk polymer when the AC frequency $\omega > \omega_c$ and certainly not the 20 -30 μm allowed in [14]. In this case the displacement of the space charge can be described as in Figure 12 a –b. It should be noted that it is not necessary for charge carriers to recombine in order to produce the displacement, only that a region around the tips reaches a state of net neutrality. When the needle polarity reverses some of the injected electrons will be in shallow traps and will be available as seed electrons for back discharges in the tree tube, but other electrons will be held in deep traps such as benzene rings in the phenoxy group of the DGBEA, which have an electron affinity of 2.253eV [31]. Other electrons taking part in damage processes will have ionized, or attached to, molecular moieties along the damage track of about 10 μm. These charges will be retained over several ac cycles, (Figure12c), as found experimentally [28], and they will continue to inhibit same polarity discharges in the same tree tube for some time.

In contrast when $\omega < \omega_c$ charge separation during a half-cycle by means of the QDC process can extend over a distance $\xi > \xi_c$, with ξ related to $(\omega_c)^{-1}$. This displaces the space charge deeper into the bulk polymer as in Figure 12 d-f. As result subsequent discharges in the same tube are much less affected and the damage generation is much more likely to take place along the same tree-tip-plane direction as initially. In this case tree tips are likely to develop new branches only at the leading parts of the tree with less bifurcations giving a tree with less branches, i.e., a lower fractal dimension. Since the branch forming damage is now concentrated along only a few directions the tree growth rate will also become greater.

The above considerations show that the relationship between tree shape, propagation time, ω_c, and tanδ, expressed in Tables 1, 2, 5, and Figs 7, 8, are due to the extent of the penetration of discharge injected space charge during a half-cycle of the applied field. It is interesting to note that in polyethylene increasing the field frequency ω for the same conditions of voltage and temperature results in a cross-over from branch trees to bush trees, and on varying the pin voltage the cross-over from branch trees to bush trees moves to low voltages with increasing frequency [41] consistent with the picture presented here.

Eventually ω_c becomes so much bigger than ω that the QDC carries a substantial amount of charge deep into the polymer bulk during the half-cycle. This will occur at high temperature, or when a high moisture content converts the percolation system into a DC conductance. In this case dielectric and joule heating may become large enough to generate a thermal runaway process leading to breakdown such as is found in Figures 7d and 8d. A possible criterion for this to occur is when ω is so large with respect to ω_c that charge separation over the percolation path extends between the tip and the plane electrode, in which case the QDC acts like a DC conductance even though the percolation system has not reached the percolation limit for an infinite cluster [42].

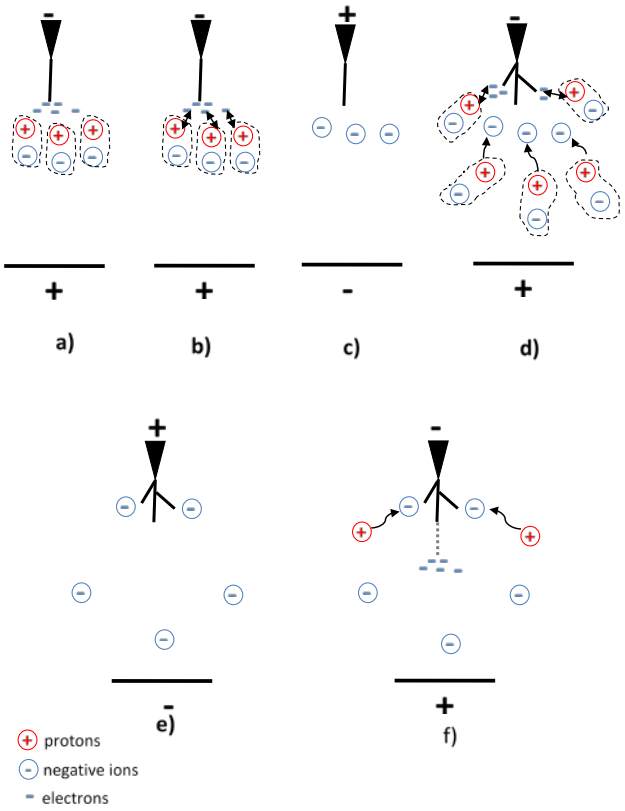

Figure 12. A qualitative description of space charge displacement around discharging electrical trees in flexible epoxy resins following a tree discharge depositing negative charge around the tree tip.

5 CONCLUSION

The shape and growth rate of electrical trees in epoxy resins has been correlated with their bulk electrical properties, and in particular with the way in which these are affected by temperature and absorbed moisture; increases in both of which have been shown to affect the electrical tree growth in a similar way. The growth time and fractal dimensions of the trees have been found to decrease with increasing temperature and/or moisture concentration. These observations were explained as the result of the effective transfer into the bulk material of the space charge deposited at the tips of the electrical tree due to the PD activity. Dielectric response measurements have shown that at lower temperature and moisture content the charge transport mechanism had a QDC form arising from a percolation type process. In this case the crucial factor is the relationship between the frequency at which long range transport sets in and the frequency of the applied field.

Levels of absorbed moisture and temperature were identified at which the degradation mechanism (electrical treeing) changes to thermal breakdown. This transition to thermal breakdown has been tentatively explained as due to the formation of percolation paths that extend over the entire distance between the pin and the plane electrodes. It is suggested that at these conditions, the loss tangent exceeds unity ($\tan\boldsymbol{\delta}>1$) at the frequency of the applied field, i.e. the dielectric loss (ε'') exceeds the charge storage capacity (ε') of the material.

REFERENCES

[1] L. A. Dissado and J. C. Fothergill, Electrical Degradation and Breakdown in Polymers, Peter Peregrinus Ltd., 1992.

[2] Y. Suzuoki, T. Saito, F. Komori, and K. Uchida, "Inception of Electrical Tree from Water-Tree Degradation," presented at the ICPADM 2006, Bali, Indonesia, pp. 111-114, 2006.

[3] L. A. Dissado, "Understanding Electrical Trees in Solids: From Experiment to Theory," IEEE Trans. Dielectrics and Electrical Insulation, vol. 9, pp. 483-497, 2002.

[4] J. V. Champion and S. J. Dodd, "Simulation of partial discharges in conducting and non-conducting electrical tree structures," J. Phys. D: Appl. Phys., vol. 34, pp. 1235-1242, 2001.

[5] J. V. Champion and S. J. Dodd, "Systematic and reproducible partial discharge patterns during electrical tree growth in an epoxy resin," J. Phys. D: Appl. Phys., vol. 29, pp. 862-868, 1996.

[6] J. V. Champion, S. J. Dodd, and G. C. Stevens, "Analysis and modelling of electrical tree growth in synthetic resins over a wide range of stressing voltage," J. Phys. D: Appl. Phys., vol. 27, pp. 1020-1030, 1994.

[7] D. W. Auckland, J. M. Cooper, and B. R. Varlow, "Factors affecting electrical tree testing," IEE Proc. - A, vol. 139, pp. 9-13, 1992.

[8] J. V. Champion and S. J. Dodd, "The effect of material composition and temperature on electrical tree growth in epoxy resins," presented at the Eighth International Conference on Dielectric Materials, Measurements and Applications Edinburgh, UK, 17-21 Sept, pp.30-34, 2000.

[9] J. V. Champion and S. J. Dodd, "An assessment of the effect of externally applied mechanical stress and water absorption on the electrical tree growth behaviour in glassy epoxy resins," J. Phys. D: Appl. Phys., vol. 32, pp. 305-316, 1999.

[10] M. D. Noskov, A. S. Malinovski, M. Sack, and A. J. Schwab, "Self-Consistent Modeling of Electrical Tree Propagation and PD Activity," IEEE Trans. Dielectrics and Electrical Insulation, vol. 7, pp. 725-733, 2000.

[11] M. D. Noskov, A. S. Malinovski, M. Sack, and A. J. Schwab, "Numerical Investigation of Insulation Conductivity Effect on Electrical Treeing," in 1999 Conference on Electrical Insulation and Dielectric Phenomena, pp. 597-600, 1999.

[12] L. A. Dissado and P. J. J. Sweeney, "Physical model for breakdown structures in solid dielectrics," Phys. Rev. B, vol. 48, pp. 16261-16268, 1993.

[13] L. A. Dissado, S. J. Dodd, J. V. Champion, P. I. Williams, and J. M. Alison, "Propagation of Electrical Tree Structures in Solid Polymeric Insulation," IEEE Trans. Dielectrics and Electrical Insulation, vol. 4, pp. 259-279, 1997.

[14] L. A. Dissado, J. C. Fothergill, N. Wise, A. Willby, and J. Cooper, "A deterministic model for branched tree structures in the electrical breakdown of solid polymeric dielectrics," J. Phys. D: Appl. Phys., vol. 33, pp. L109-L112, 2000.

[15] S. J. Dodd, "A deterministic model for the growth of non-conducting electrical tree structures," J. Phys. D: Appl. Phys., vol. 36, pp. 129-141, 2003.

[16] J. V. Champion and S. J. Dodd, "Charge dynamics during electrical treeing measured using a bridge system", in Space Charge in Solid Dielectrics, Dielectric Society: Leicester, 1998, pp. 273-284

[17] N. M. Chalashkanov, S. J. Dodd, L. A. Dissado, and J. C. Fothergill, "Re-examination of the dielectric spectra of epoxy resins: bulk charge transport and interfacial polarization peaks " IEEE Transactions on Dielectrics and Electrical Insulation, vol. 21, pp. 1330-1341, 2014.

[18] N. M. Chalashkanov, S. J. Dodd, J. C. Fothergill, and L. A. Dissado, "On the Relationship between Bulk Charge Transport and Electrical Breakdown Mechanisms in Epoxy Resins," presented at the Nord-IS 11, Tampere, 2011.

[19] L. Greenspan, "Humidity Fixed Points of Binary Saturated Aqueous Solutions," Journal of Research of the National Bureau of Standards - A. Physics and Chemistry, vol. 81A, pp. 89-96, 1977.

[20] OIML, "The scale of relative humidity of air certified against saturated salt solutions," Oraganisation Internationale de Metrologie Legale, 1996.

[21] L. A. Dissado and R. M. Hill, "Anomalous Low-frequency Dispersion," J. Chem. Soc., Faraday Trans. 2, vol. 80, pp. 291-319, 1984.

[22] A. K. Jonscher, Dielectric relaxation in solids, Chelsea Dielectrics Press: London, 1983.

[23] A. K. Jonscher, Universal relaxation law, Chelsea Dielectrics Press: London, 1996.

[24] M. Shablakh, L. A. Dissado, and R. M. Hill, "Nonconductive Long-Range Charge Transport in Hydrated Biopolymers," Journal of Biological Physics, vol. 12, pp. 63-78, 1984.

[25] P. M. Suherman, P. Taylor, and G. Smith, "Low frequency dielectric study on hydrated ovalbumin," Journal of Non-Crystalline Solids, vol. 305, pp. 317-321, 2002.

[26] P. M. Suherman and G. Smith, "A percolation cluster model of the temperature dependent dielectric properties of hydrated proteins," J. Phys. D: Appl. Phys., vol. 36, pp. 336-342, 2003.

[27] V. Griseri, The effect of high electric fields on an epoxy resin, PhD thesis., Department of Engineering, University of Leicester, Leicester, 2000.

[28] N. Chalashkanov, Influence of Water Absorption and Temperature on Charge Transport and Electrical Degradation in Epoxy Resins, PhD thesis, Department of Engineering, University of Leicester, 2011.

[29] D. Marx, "Proton Transfer 200 Years after von Grotthuss: Insights from Ab Initio Simulations," ChemPhysChem, vol. 7, pp. 1848-1870, 2006.

[30] S. Popineau, C. Rondeau-Mouro, C. Sulpice-Gaillet, and M. E. R. Shanahan, "Free/bound water absorption in an epoxy adhesive," Polymer, vol. 46, pp. 10733-10740, 2005.

[31] CRC handbook of chemistry and physics / David R. Lide, editor-in-chief. Version 2008 ed. London: CRC Press, 2008.

[32] L. Flandin, L. Vouyovitch, A. Beroual, J.-L. Bessede, and N. D. Alberola, "Influences of degree of curing and presence of inorganic fillers on the ultimate electrical properties of epoxy-based composites: experiment and simulation " J. Phys. D: Appl. Phys., vol. 38, pp. 144-155, 2005.

[33] S. J. Dodd, N. Chalashkanov, and J. C. Fothergill, "Statistical Analysis of Partial Discharges from Electrical Trees Grown in a Flexible Epoxy Resin," presented at the Proc. IEEE - CEIDP 2008, Quebec city, Canada, October 26-29, pp. 666 – 669, 2008.

[34] N. Chalashkanov, S. J. Dodd, L. A. Dissado, and J. C. Fothergill, "Pulse Sequence Analysis on PD data from electrical trees in flexible epoxy resins," presented at the CEIDP 2011, Cancun, Mexico, October 16-19, pp. 776 – 779, 2011.

[35] J. Sletbak, N. G. Gjelsten, E. E. Henriksen, and T. J. Lanoue, "Influence of moisture on permittivity and dielectric losses in cast epoxy systems," presented at the Nord-IS 88, Trondheim, Norway, pp. 19/1-10, 1988.

[36] H. C. Hall and R. M. Russek, "Discharge Inception and Extinction in Dielectric Voids," Proc. IEE, vol. 101, pp. 47-55, 1954.

[37] L. A. Dissado and R. M. Hill, "The fractal nature of the cluster model dielectric response functions," Journal of Applied Physics, vol. 66, pp. 2511-2524, 1989.

[38] L. A. Dissado, "A fractal interpretation of the dielectric response of animal tissues," Phys. Med. Biol., vol. 35, pp. 1487-1503, 1990.

[39] R. M. Hill, L. A. Dissado, and R. R. Nigmatullin, "Invariant behaviour classes for the response of simple fractal circuits," J. Phys. Condens. Matter, vol. 3, pp. 9773-9790, 1991.

[40] S. J. Dodd, L. A. Dissado, J. V. Champion, and J. M. Alison, "Evidence for deterministic chaos as the origin of electrical tree breakdown structures in polymeric insulation," Physical Review B, vol. 52, pp. R16 985-R16 988, 1995.

[41] F. Noto and N. Yoshimura, "Voltage and Frequency Dependence of Tree Growth in Polyethylene," presented at the Ann. Rep. CEIDP, pp. 207-217, 1974.

[42] D. Stauffer and A. Aharony, Introduction to Percolation Theory, 2nd ed., Taylor&Francis Ltd, 1994.

Nikola M. Chalashkanov (M'07) was born in Sofia, Bulgaria in 1981. He graduated from the Technical University of Sofia in 2003 with a Bachelor's degree in industrial engineering and gained the Master's degree there in industrial engineering in 2005. He joined the University of Leicester, UK in 2007 as a Teaching Assistant and received a Ph.D. degree in Charge transport and electrical breakdown in epoxy resins in 2012. He is currently a Teaching Fellow in the Electrical Power and Power Electronics Research Group in the Department of Engineering, University of Leicester. His research interests include partial discharge and electrical treeing phenomena, dielectric properties and charge transport in polymers, chaos theory, statistical analysis and data mining. He is a member of IoP.

Stephen J. Dodd (M'11) was born in Harlow, Essex in 1960. He received the B.Sc. (Hons) physics degree in 1987 and the Ph.D. degree in physics in 1992, both from London Guildhall University, UK and remained at the University until 2002 as a Research Fellow. He joined the University of Southampton in

2002 as a Lecturer in the Electrical Power Engineering Group in the School of Electronics and Computer Science and then the University of Leicester in the Electrical Power and Power Electronics Research Group in the Department of Engineering in 2007 as a Senior Lecturer. His research interests lie in the areas of light scattering techniques for the characterization of polymer morphology, electrical treeing breakdown process in polymeric materials and composite insulation materials, electroluminescence and its relationship with electrical and thermal ageing of polymers, characterization of liquid and solid dielectrics and condition monitoring and assessment of high voltage engineering plant.

Leonard A Dissado (F'06) He was born in St. Helens, Lancashire, U.K. on 29 August 1942. He was educated at Thomas Linacre Technical School, Wigan, Lancashire during 1953-1960, gaining a State Scholarship for University Entry in 1959. He graduated from University College, London, with a 1st Class degree in chemistry in 1963 and was awarded a Ph.D. degree in theoretical chemistry in 1966 and the D.Sc. degree in 1990. After rotating between Australia and England twice he settled in at Chelsea College in 1977 to carry out research into dielectrics. His interest in breakdown and associated topics started with a consultancy with STL that begun in 1981. Since then he has published many papers and one book, together with John Fothergill, in this area. In 1995 he moved to The University of Leicester, and was promoted to Professor in 1998, and is now Professor Emeritus. He has been a visiting Professor at The University Pierre and Marie Curie in Paris, Paul Sabatier University in Toulouse, Nagoya University, and NIST at Boulder Colorado. He has given numerous invited lectures, including the E.O. Forster (ICSD 2001) and the Whitehead memorial lecture (CEIDP 2002). Currently he is an Associate Editor of IEEE Transactions DEI and was Chairman of the DEIS Publications Committee. He was awarded the degree Doctuer Honoris Causa by the Universite Paul Sabatier, Toulouse in October 2007, and a Honorary Professorship of Xian Jiaotong University, China, in 2008, where he gives a masters course on 'The physics of insulating polymers' each autumn.

John Fothergill (F'05) was born in Malta in 1953. He graduated from the University of Wales, Bangor, in 1975 with a Batchelor's degree in Electronic Engineering. He continued at the same institution, working with Pethig and Lewis, gaining a Master's degree in Electrical Materials and Devices in 1976 and doctorate in the Electronic Properties of Biopolymers in 1979. Following this he worked as a senior research engineer leading research in electrical power cables at STL, Harlow, UK. In 1984 he moved to the University of Leicester as a lecturer, where he subsequently became a Professor and eventually Pro-Vice-Chancellor. He moved to City, University of London in August 2012 to become Pro-Vice-Chancellor for research and enterprise. He is now Professor Emeritus at City, University of London, a Visiting Professor at the University of Leicester, and works as a consultant.